Sodium Ion Batteries

Deutsche Ausgabe: DOI: 10.1002/ange.201606508
Internationale Ausgabe: DOI: 10.1002/anie.201606508

An Aqueous Symmetric Sodium-Ion Battery with NASICON-Structured $Na_3MnTi(PO_4)_3$

*Hongcai Gao and John B. Goodenough**

Abstract: *A symmetric sodium-ion battery with an aqueous electrolyte is demonstrated; it utilizes the NASICON-structured $Na_3MnTi(PO_4)_3$ as both the anode and the cathode. The NASICON-structured $Na_3MnTi(PO_4)_3$ possesses two electrochemically active transition metals with the redox couples of Ti^{4+}/Ti^{3+} and Mn^{3+}/Mn^{2+} working on the anode and cathode sides, respectively. The symmetric cell based on this bipolar electrode material exhibits a well-defined voltage plateau centered at about 1.4 V in an aqueous electrolyte with a stable cycle performance and superior rate capability. The advent of aqueous symmetric sodium-ion battery with high safety and low cost may provide a solution for large-scale stationary energy storage.*

The development of electric-power storage devices, with the characteristics of low cost, high-energy-density, and long cycle life, is a global priority to integrate renewable and clean electric-power generated from solar and wind energy into a smart electrical grid.[1–3] Despite the great achievement of lithium-ion batteries in portable electronics and electric vehicles in recent years, the insufficient and unevenly distributed lithium resources as well as increasing cost may restrict their application in large-scale electrical energy storage systems.[4–7] Consequently, extensive efforts have been devoted to the investigation of sodium-ion batteries with nonaqueous electrolytes that share similar scientific and technological principles to the commercialized lithium-ion batteries.[8–13] Although the utilization of organic liquid electrolytes enables sodium-ion batteries with a higher voltage and a wider choice of electrode materials, safety and environmental concerns are arising from the toxic and flammable organic solvents.[14,15] Furthermore, compared with aqueous electrolytes, the much lower ionic conductivities and higher costs of organic liquid electrolytes possibly impose additional constrains on large-scale application of nonaqueous sodium-ion batteries. To overcome the drawbacks of organic liquid electrolytes, the development of sodium-ion batteries with aqueous electrolytes may represent a promising approach for large-scale storage of electrical energy.[16–19]

Recently, a number of transition metal oxides, Prussian blue analogues, and polyanionic frameworks have demonstrated stable sodium storage performance in aqueous electrolytes.[20–24] Particular interests have also been focused on sodium storage in NASICON (Na Super Ionic Conductors)-type compounds because of their structural stability, their large ionic channels, and the abundance of sodium-insertion sites.[25–27] The NASICON-structured materials with the formula unit of $A_xM_y(XO_4)_3$, where A, M and X are alkali metal, transition metal and nonmetal atoms, respectively, can be described as three-dimensional polyanionic frameworks of corner sharing MO_6 octahedra and XO_4 tetrahedra with interconnected channels for the diffusion of alkali ions.[28,29] The redox potentials of NASICON-structured materials can be tuned by changing the elemental composition and/or the valence states of the transition metal ions.[30] The NASICON-structured $NaTi_2(PO_4)_3$ has a sodium-ion insertion potential well-above the evolution of H_2 in an aqueous Na_2SO_4 electrolyte.[31] The recently synthesized $Na_3Ti_2(PO_4)_3$ as a sodium-bearing anode for aqueous sodium-ion batteries enables the utilization of sodium-depleted cathode materials.[32] Sodium-ion full-cells with aqueous electrolytes were also constructed with the $NaTi_2(PO_4)_3$ anode and a variety of cathodes, including $Na_{0.44}MnO_2$,[33] $Na_2NiFe(CN)_6$,[34] $Na_2CuFe(CN)_6$,[35] $Na_3V_2(PO)_4$,[36] and $NaMnO_2$.[37]

In this work, a NASICON-type compound of $Na_3MnTi(PO_4)_3$ was prepared to construct an aqueous symmetric sodium-ion battery. The design of a symmetric battery is attractive because the cathode and anode with the same active material can simplify the fabrication process, reduce the manufacturing costs, and buffer the volume change of electrodes (the cathode shrinking accompanied by anode expansion, and vice versa).[38,39] Recently, the layered metal oxides of O3-$Na_{0.8}Ni_{0.4}Ti_{0.6}O_2$ and P2-$Na_{0.66}Ni_{0.17}Co_{0.17}Ti_{0.66}O_2$ were successfully used to realize symmetric sodium-ion batteries through the utilization of the redox centers of nickel and cobalt on the cathode side and titanium on the anode side in organic liquid electrolytes.[40,41] The realization of an aqueous symmetric sodium-ion battery requires the discovery of an electrode material that can be used as a sodium-rich cathode and a sodium-deficient anode, with sufficient sodium storage capacities, reversible redox activities, and especially working within the electrochemical potential window of water (within the oxygen and hydrogen evolution potentials). The NASICON-type $Na_3MnTi(PO_4)_3$ forms a three-dimensional framework based on MnO_6 or TiO_6 octahedra sharing all of its corners with PO_4 tetrahedra (Figure 1). Two independent types of sodium ions are located in the interstitial sites of the framework with two different oxygen environments: A single interstitial site per formula unit with six-fold coordination (M1 site) is occupied by a less-mobile sodium-ion, and three equivalent sites per formula unit with eight-fold coordination (M2 sites) are occupied by two mobile sodium-ions. Since the sodium ions positioned at

[*] Dr. H. C. Gao, Prof. J. B. Goodenough
Texas Materials Institute, The University of Texas at Austin
Austin, Texas 78712 (USA)
E-mail: jgoodenough@mail.utexas.edu

Supporting information for this article can be found under: http://dx.doi.org/10.1002/anie.201606508.

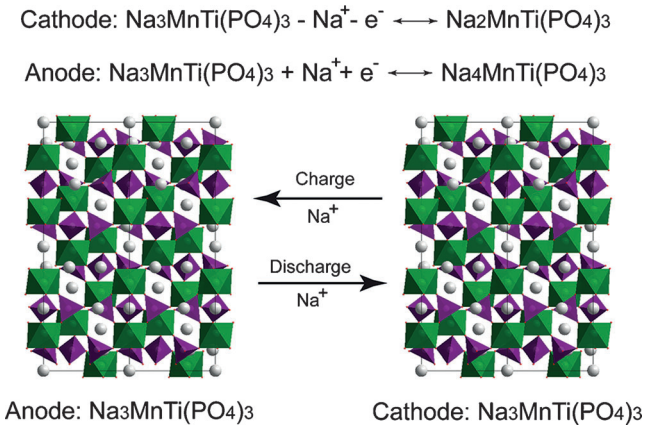

Figure 1. Schematic illustration of the aqueous symmetric sodium-ion battery with the NASICON-structured $Na_3MnTi(PO_4)_3$ as the anode and the cathode.

M1 sites are strongly bound to the coordinated oxygen atoms, only the sodium ions residing at M2 sites can be extracted/inserted for electrochemical activity.[42] We demonstrated that the extraction of one sodium-ion per formula unit from $Na_3MnTi(PO_4)_3$ with the formation of $Na_2MnTi(PO_4)_3$ through the Mn^{3+}/Mn^{2+} redox couple is well-below the oxygen evolution potential, and the insertion of one sodium-ion per formula unit into $Na_3MnTi(PO_4)_3$ with the formation of $Na_4MnTi(PO_4)_3$ through the Ti^{4+}/Ti^{3+} redox couple is well-above the hydrogen evolution potential in the neutral aqueous electrolyte of Na_2SO_4 (1.0 M). Therefore, $Na_3MnTi(PO_4)_3$ enables its utilization as both a sodium-rich cathode and a sodium-deficient anode for a symmetric sodium-ion battery in the aqueous electrolyte.

$Na_3MnTi(PO_4)_3$ was synthesized by a sol-gel method followed by calcination of the precursor at 600 °C in argon atmosphere. The XRD diffraction pattern (Figure 2) of $Na_3MnTi(PO_4)_3$ can be indexed into a rhombohedral NASICON-type unit cell with the $R\bar{3}c$ space group (Table S1, Supporting Information). The morphology of $Na_3MnTi(PO_4)_3$ was analyzed by scanning electron microscopy (SEM) and transmission electron microscopy (TEM). SEM images showed that the particle size of $Na_3MnTi(PO_4)_3$ ranges from a few hundreds of nanometers to several micrometers. TEM images revealed that the $Na_3MnTi(PO_4)_3$ particles are composed of nanosized primary particles well-dispersed in a carbon matrix. The presence of carbon is used to improve the electrical conductivity of $Na_3MnTi(PO_4)_3$. The carbon content is about 7.8 wt.%, determined by thermogravimetric analysis (TGA) of the $Na_3MnTi(PO_4)_3$ sample. The chemical composition of $Na_3MnTi(PO_4)_3$ was confirmed by energy-dispersive X-ray spectroscopy (EDS) analysis (Figure S1, Supporting Information).

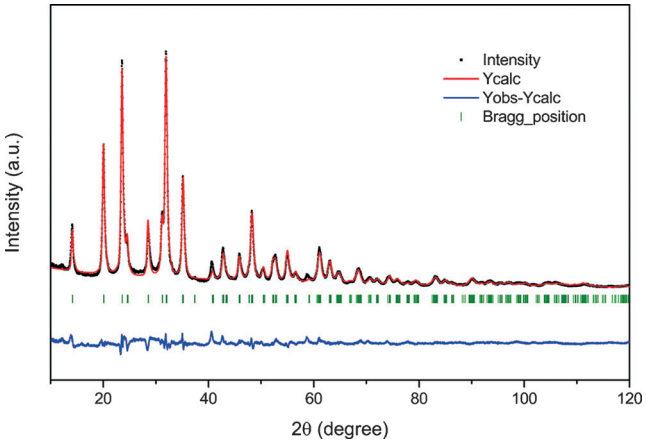

Figure 2. X-ray diffraction pattern and Rietveld refinement of $Na_3MnTi(PO_4)_3$.

The electrochemical properties of $Na_3MnTi(PO_4)_3$ as a bipolar electrode material were first assessed in a three-electrode system with Ag/AgCl as the reference electrode in the aqueous electrolyte of Na_2SO_4 (1.0 M). The cyclic voltammogram (CV) of the $Na_3MnTi(PO_4)_3$ electrode features a pair of redox peaks centered at about 0.6 V vs. Ag/AgCl (Figure 3 A), which can be attributed to the reversible reactions of the Mn^{3+}/Mn^{2+} redox couple in the NASICON lattice with extraction/insertion of sodium-ions from/into $Na_3MnTi(PO_4)_3$. The redox voltage of Mn^{3+}/Mn^{2+} in the NASICON-structured $Na_3MnTi(PO_4)_3$ is well-below the oxygen evolution potential in the neutral aqueous electrolyte (1.1 V vs. Ag/AgCl), which therefore enables it to be used as a high-voltage cathode for aqueous sodium-ion batteries.[43–45] In accordance with the CV results, the $Na_3MnTi(PO_4)_3$ electrode exhibited

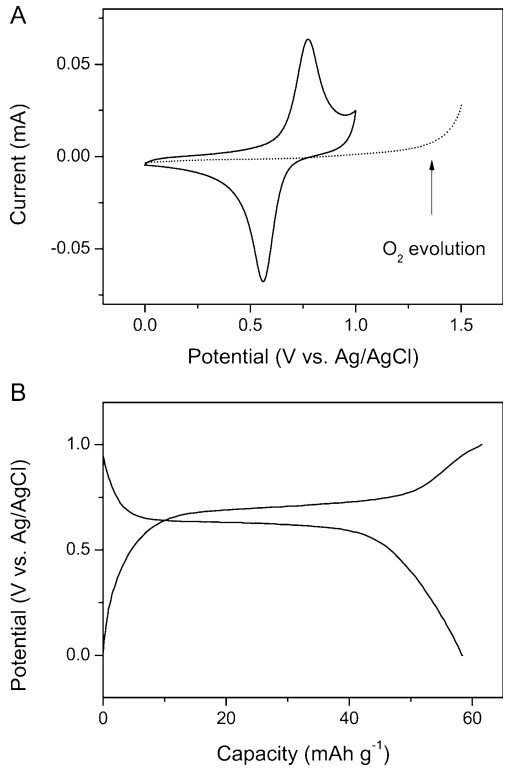

Figure 3. The electrochemical performance of $Na_3MnTi(PO_4)_3$ for the Mn^{3+}/Mn^{2+} redox couple in a three-electrode system with Ag/AgCl as the reference electrode. A) The cyclic voltammogram of $Na_3MnTi(PO_4)_3$ (solid line) and the linear sweep voltammogram of the activated carbon electrode (dot line) at a scan rate of 1.0 mV^{-1} s. B) The galvanostatic charge/discharge profiles of $Na_3MnTi(PO_4)_3$ between 0 V and 1.0 V at a rate of 0.5 C.

charge and discharge profiles with well-defined voltage plateaus centered at about 0.6 V vs. Ag/AgCl with little polarization (Figure 3B), corresponding to the reversible reaction of $Na_3MnTi(PO_4)_3 - Na^+ - e^- \rightleftarrows Na_2MnTi(PO_4)_3$, with the oxidation of Mn^{2+} to Mn^{3+} on charge and the reduction of Mn^{3+} to Mn^{2+} on discharge,[46,47] keeping the valence state of Ti^{4+} unchanged (Figure S2, Supporting Information). The $Na_3MnTi(PO_4)_3$ electrode delivers a discharge capacity of 58.4 mAh g^{-1} at a rate of 0.5 C (1 C = 58.7 mA g^{-1}), corresponding to a nearly 100% utilization of its one sodium extraction/insertion capacity of the $Na_3MnTi(PO_4)_3$ electrode through the Mn^{3+}/Mn^{2+} redox couple. The structural change of $Na_3MnTi(PO_4)_3$ is reversible during extraction and insertion of one sodium-ion per formula unit through the Mn^{3+}/Mn^{2+} redox couple. When charging the electrode to 1.0 V vs. Ag/AgCl, the X-ray diffraction peaks of (012), (113), (024), and (300) shift to higher angles, indicative of a volume shrinkage because of the extraction of sodium ions from the NASICON-structured material.[48] Upon discharging to 0 V vs. Ag/AgCl, the diffraction peaks of the electrode recovered to its original state (Figure S3, Supporting Information).

The redox couple of Ti^{4+}/Ti^{3+} in the NASICON-structured $Na_3MnTi(PO_4)_3$ was also evaluated in a three-electrode system in the aqueous electrolyte of Na_2SO_4 (1.0 M). The main feature of the CV curves of $Na_3MnTi(PO_4)_3$ is a pair of redox peaks centered at about −0.8 V vs. Ag/AgCl (Figure 4A), corresponding to the reversible insertion/extraction reaction of one sodium-ion per formula unit into/from the $Na_3MnTi(PO_4)_3$ lattice operating in a reversible reaction of $Na_3MnTi(PO_4)_3 + Na^+ + e^- \rightleftarrows Na_4MnTi(PO_4)_3$. The observed voltage of the Ti^{4+}/Ti^{3+} redox couple in $Na_3MnTi(PO_4)_3$ is in accordance with the voltage of the Ti^{4+}/Ti^{3+} redox couple in $NaTi_2(PO_4)_3$, which is sufficiently higher than the hydrogen evolution potential in the neutral aqueous electrolyte (−1.2 V vs. Ag/AgCl).[49,50] The galvanostatic discharge/charge profiles revealed that the $Na_3MnTi(PO_4)_3$ electrode delivers a sodiation capacity of 58.2 mAh g^{-1} at a rate of 0.5 C, corresponding to almost full utilization of the Ti^{4+}/Ti^{3+} redox couple in $Na_3MnTi(PO_4)_3$, with the reduction of Ti^{4+} to Ti^{3+} upon the insertion of one sodium-ion per formula unit and the oxidation of Ti^{3+} to Ti^{4+} upon the extraction of the inserted sodium-ion, without changing the valence state of Mn^{2+} (Figure S4, Supporting Information).[51,52] In addition, the charge and discharge reaction of $Na_3MnTi(PO_4)_3$ proceeded mostly at a flat plateau centered at about −0.8 V vs. Ag/AgCl without significant polarization, suggesting an excellent electrochemical reversibility of the $Na_3MnTi(PO_4)_3$ electrode (Figure 4B). When discharging the electrode to −1.3 V vs. Ag/AgCl, the X-ray diffraction peaks of (113), (024), (211), and (300) shift to lower angles, because of a volume expansion after the insertion of sodium-ions into the NASICON-structured material.[53] After the extraction of the inserted sodium-ions, the material transforms back completely to its original phase (Figure S5, Supporting Information).

Since the sodium-ion insertion/extraction reactions through the Mn^{3+}/Mn^{2+} and Ti^{4+}/Ti^{3+} redox couples in $Na_3MnTi(PO_4)_3$ take place within the electrochemical window of the aqueous electrolyte, it is thus expected a symmetric sodium-ion battery with $Na_3MnTi(PO_4)_3$ as the cathode and the anode would have a high capacity utilization and a stable cycling performance in the aqueous electrolyte of Na_2SO_4 (1.0 M). Furthermore, the combination of the Mn^{3+}/Mn^{2+} and Ti^{4+}/Ti^{3+} redox couples in $Na_3MnTi(PO_4)_3$ would enable the symmetric battery to possess a high output voltage of approximately 1.4 V. Figure 5A illustrates the CV curve of the symmetric cell within the voltage of 0.4 V and 1.8 V in the aqueous electrolyte. The oxidation and reduction peaks were centered at about 1.4 V, which is consistent with the predicted value on the basis of the voltage difference between the Mn^{3+}/Mn^{2+} and Ti^{4+}/Ti^{3+} redox couples in $Na_3MnTi(PO_4)_3$. As shown in Figure 5B, the charge/discharge profiles of the symmetric cell are centered at about 1.4 V without obvious polarization, delivering a reversible capacity of 57.9 mAh g^{-1} at a charge/discharge rate of 0.5 C. The energy density of the symmetric cell is about 40 Wh kg^{-1} based on the total weight of the active materials in the anode and cathode, which is comparable to or higher than the conventional aqueous rechargeable batteries and the recently developed aqueous sodium-ion batteries (Table S2, Supporting Information). The rate capability of the symmetric cell is also evaluated at different charge/discharge rates from 0.5 C to 10 C (Figure 5C). The reversible capacity of the symmetric cell was 56.5 mAh g^{-1} at the rate of 1 C, and 46.7 mAh g^{-1} at the rate of 10 C. When the rate was back to 0.5 C, the capacity of 57.8 mAh g^{-1} was recovered, demonstrating an excellent rate

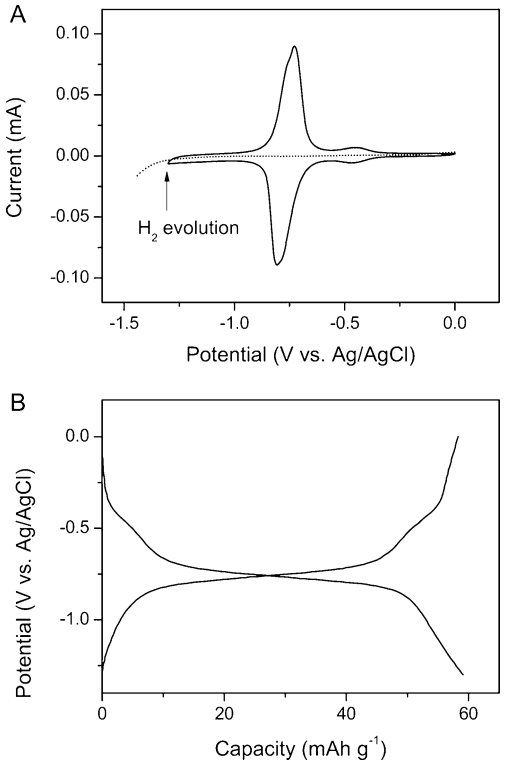

Figure 4. The electrochemical performance of $Na_3MnTi(PO_4)_3$ for the Ti^{4+}/Ti^{3+} redox couple in a three-electrode system with Ag/AgCl as the reference electrode. A) The cyclic voltammogram of $Na_3MnTi(PO_4)_3$ (solid line) and the linear sweep voltammogram of the activated carbon electrode (dot line) at a scan rate of 1.0 mV^{-1} s. B) The galvanostatic charge/discharge profiles of $Na_3MnTi(PO_4)_3$ between −1.3 V and 0 V at a rate of 0.5 C.

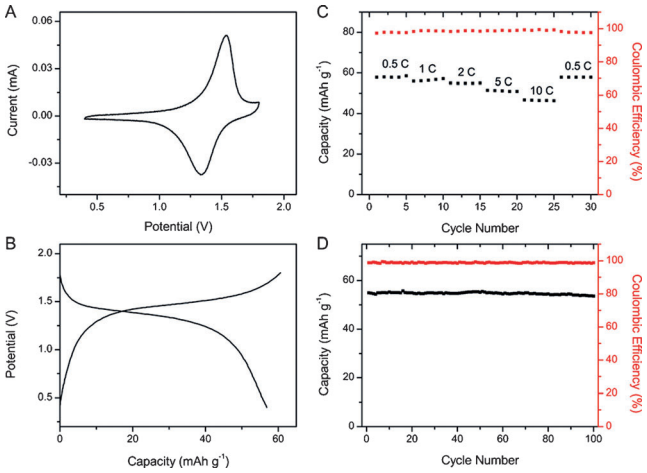

Figure 5. The electrochemical performance of the symmetric sodium-ion battery with $Na_3MnTi(PO_4)_3$ as the anode and cathode in an aqueous electrolyte. A) The cyclic voltammogram of the symmetric sodium-ion battery between 0.4 V and 1.8 V at a scan rate of 1.0 mV^{-1} s. B) The charge/discharge profiles of the symmetric sodium-ion battery between 0.4 V and 1.8 V at a rate of 0.5 C. C) The rate performance of the symmetric sodium-ion battery at different rates from 0.5 C to 10 C. D) The capacity retention and coulombic efficiency of the symmetric sodium-ion battery at a rate of 1 C.

capability of the symmetric cell. Importantly, about 98% of its initial capacity can be retained for the symmetric battery after 100 charge/discharge cycles at a rate of 1 C (Figure 5D), with the coulombic efficiency exceeding 99% in the charge/discharge cycles, manifesting the high reversibility of the symmetric cell through the Mn^{3+}/Mn^{2+} and Ti^{4+}/Ti^{3+} redox couples on the cathode and anode sides, respectively, in the NASICON-structured $Na_3MnTi(PO_4)_3$.

In conclusion, with the application of a low-cost bipolar electrode material of NASICON-structured $Na_3MnTi(PO_4)_3$, a symmetric sodium-ion battery with an aqueous electrolyte was constructed to meet the demand of stationary energy storage. The symmetric sodium-ion battery exhibits an operating voltage of 1.4 V in the aqueous electrolyte of Na_2SO_4 with an excellent rate capability and cycle stability. The development of aqueous symmetric sodium-ion batteries with a low cost, long cycle life, high safety, high efficiency, and an environmentally-benign nature may pave the way for large-scale stationary energy storage applications and will provide new opportunities towards the advancement of room-temperature sodium-ion batteries.

Acknowledgements

The synthesis, analysis, and electrochemical characterization of the electrode material were supported by the US Department of Energy, Office of Basic Energy Sciences (Grant number DE-SC0005397). J.B.G. also acknowledges support from the Robert A. Welch Foundation (Grant F-1066).

Keywords: aqueous electrolyte · energy storage · sodium-ion battery · symmetric battery

[1] M. Armand, J. M. Tarascon, *Nature* **2008**, *451*, 652–657.
[2] J. B. Goodenough, *Acc. Chem. Res.* **2013**, *46*, 1053–1061.
[3] B. Scrosati, J. Garche, *J. Power Sources* **2010**, *195*, 2419–2430.
[4] M. S. Whittingham, *Chem. Rev.* **2004**, *104*, 4271–4301.
[5] J. B. Goodenough, K. S. Park, *J. Am. Chem. Soc.* **2013**, *135*, 1167–1176.
[6] Z. G. Yang, J. L. Zhang, M. C. W. Kintner-Meyer, X. C. Lu, D. W. Choi, J. P. Lemmon, J. Liu, *Chem. Rev.* **2011**, *111*, 3577–3613.
[7] D. Kundu, E. Talaie, V. Duffort, L. F. Nazar, *Angew. Chem. Int. Ed.* **2015**, *54*, 3431–3448; *Angew. Chem.* **2015**, *127*, 3495–3513.
[8] N. Yabuuchi, M. Kajiyama, J. Iwatate, H. Nishikawa, S. Hitomi, R. Okuyama, R. Usui, Y. Yamada, S. Komaba, *Nat. Mater.* **2012**, *11*, 512–517.
[9] M. H. Han, E. Gonzalo, G. Singh, T. Rojo, *Energy Environ. Sci.* **2015**, *8*, 81–102.
[10] L. Wang, Y. H. Lu, J. Liu, M. W. Xu, J. G. Cheng, D. W. Zhang, J. B. Goodenough, *Angew. Chem. Int. Ed.* **2013**, *52*, 1964–1967; *Angew. Chem.* **2013**, *125*, 2018–2021.
[11] Y. You, X. L. Wu, Y. X. Yin, Y. G. Guo, *Energy Environ. Sci.* **2014**, *7*, 1643–1647.
[12] P. Barpanda, G. Oyama, S. Nishimura, S. C. Chung, A. Yamada, *Nat. Commun.* **2014**, *5*, 4358.
[13] Z. L. Jian, C. C. Yuan, W. Z. Han, X. Lu, L. Gu, X. K. Xi, Y. S. Hu, H. Li, W. Chen, D. F. Chen, Y. Ikuhara, L. Q. Chen, *Adv. Funct. Mater.* **2014**, *24*, 4265–4272.
[14] W. Tang, Y. S. Zhu, Y. Y. Hou, L. L. Liu, Y. P. Wu, K. P. Loh, H. P. Zhang, K. Zhu, *Energy Environ. Sci.* **2013**, *6*, 2093–2104.
[15] X. Dong, L. Chen, X. Su, Y. Wang, Y. Xia, *Angew. Chem. Int. Ed.* **2016**, *55*, 7474–7477; *Angew. Chem.* **2016**, *128*, 7600–7603.
[16] J. F. Whitacre, S. Shanbhag, A. Mohamed, A. Polonsky, K. Carlisle, J. Gulakowski, W. Wu, C. Smith, L. Cooney, D. Blackwood, J. C. Dandrea, C. Truchot, *Energy Technol.* **2015**, *3*, 20–31.
[17] Y. Liu, Y. Qiao, W. X. Zhang, H. Wang, K. Y. Chen, H. P. Zhu, Z. Li, Y. H. Huang, *J. Mater. Chem. A* **2015**, *3*, 7780–7785.
[18] H. Kim, J. Hong, K. Y. Park, H. Kim, S. W. Kim, K. Kang, *Chem. Rev.* **2014**, *114*, 11788–11827.
[19] G. L. Li, Z. Yang, Y. Jiang, W. X. Zhang, Y. H. Huang, *J. Power Sources* **2016**, *308*, 52–57.
[20] X. L. Dong, L. Chen, J. Y. Liu, S. Haller, Y. G. Wang, Y. Y. Xia, *Sci. Adv.* **2016**, *2*, e1501038.
[21] M. Pasta, C. D. Wessells, N. Liu, J. Nelson, M. T. McDowell, R. A. Huggins, M. F. Toney, Y. Cui, *Nat. Commun.* **2014**, *5*, 3007.
[22] Y. S. Wang, J. Liu, B. J. Lee, R. M. Qiao, Z. Z. Yang, S. Y. Xu, X. Q. Yu, L. Gu, Y. S. Hu, W. L. Yang, K. Kang, H. Li, X. Q. Yang, L. Q. Chen, X. J. Huang, *Nat. Commun.* **2015**, *6*, 6401.
[23] C. D. Wessells, M. T. McDowell, S. V. Peddada, M. Pasta, R. A. Huggins, Y. Cui, *ACS Nano* **2012**, *6*, 1688–1694.
[24] Y. H. Jung, C. H. Lim, J. H. Kim, D. K. Kim, *RSC Adv.* **2014**, *4*, 9799–9802.
[25] S. Difi, I. Saadoune, M. T. Sougrati, R. Hakkou, K. Edstrom, P. E. Lippens, *J. Phys. Chem. C* **2015**, *119*, 25220–25234.
[26] K. Saravanan, C. W. Mason, A. Rudola, K. H. Wong, P. Balaya, *Adv. Energy Mater.* **2013**, *3*, 444–450.
[27] Z. L. Jian, L. Zhao, H. L. Pan, Y. S. Hu, H. Li, W. Chen, L. Q. Chen, *Electrochem. Commun.* **2012**, *14*, 86–89.
[28] J. B. Goodenough, H. Y. P. Hong, J. A. Kafalas, *Mater. Res. Bull.* **1976**, *11*, 203–220.
[29] A. Manthiram, J. B. Goodenough, *J. Power Sources* **1989**, *26*, 403–408.
[30] A. K. Padhi, K. S. Nanjundaswamy, C. Masquelier, J. B. Goodenough, *J. Electrochem. Soc.* **1997**, *144*, 2581–2586.

[31] S. I. Park, I. Gocheva, S. Okada, J. Yamaki, *J. Electrochem. Soc.* **2011**, *158*, A1067 – A1070.
[32] Z. Li, D. B. Ravnsbaek, K. Xiang, Y. M. Chiang, *Electrochem. Commun.* **2014**, *44*, 12 – 15.
[33] Z. Li, D. Young, K. Xiang, W. C. Carter, Y. M. Chiang, *Adv. Energy Mater.* **2013**, *3*, 290 – 294.
[34] X. Y. Wu, Y. L. Cao, X. P. Ai, J. F. Qian, H. X. Yang, *Electrochem. Commun.* **2013**, *31*, 145 – 148.
[35] X. Y. Wu, M. Y. Sun, Y. F. Shen, J. F. Qian, Y. L. Cao, X. P. Ai, H. X. Yang, *ChemSusChem* **2014**, *7*, 407 – 411.
[36] Q. Zhang, C. Y. Liao, T. Y. Zhai, H. Q. Li, *Electrochim. Acta* **2016**, *196*, 470 – 478.
[37] Z. G. Hou, X. N. Li, J. W. Liang, Y. C. Zhu, Y. T. Qian, *J. Mater. Chem. A* **2015**, *3*, 1400 – 1404.
[38] Y. Noguchi, E. Kobayashi, L. S. Plashnitsa, S. Okada, J. Yamaki, *Electrochim. Acta* **2013**, *101*, 59 – 65.
[39] L. S. Plashnitsa, E. Kobayashi, Y. Noguchi, S. Okada, J. Yamaki, *J. Electrochem. Soc.* **2010**, *157*, A536 – A543.
[40] S. H. Guo, H. J. Yu, P. Liu, Y. Ren, T. Zhang, M. W. Chen, M. Ishida, H. S. Zhou, *Energy Environ. Sci.* **2015**, *8*, 1237 – 1244.
[41] S. H. Guo, P. Liu, Y. Sun, K. Zhu, J. Yi, M. W. Chen, M. Ishida, H. S. Zhou, *Angew. Chem. Int. Ed.* **2015**, *54*, 11701 – 11705; *Angew. Chem.* **2015**, *127*, 11867 – 11871.
[42] W. X. Song, X. Y. Cao, Z. P. Wu, J. Chen, K. Huangfu, X. W. Wang, Y. L. Huang, X. B. Ji, *Phys. Chem. Chem. Phys.* **2014**, *16*, 17681 – 17687.
[43] Y. Liu, Y. Qiao, W. X. Zhang, H. H. Xu, Z. Li, Y. Shen, L. X. Yuan, X. L. Hu, X. Dai, Y. H. Huang, *Nano Energy* **2014**, *5*, 97 – 104.
[44] H. Manjunatha, T. V. Venkatesha, G. S. Suresh, *J. Solid State Electrochem.* **2012**, *16*, 1941 – 1952.
[45] M. Minakshi, P. Singh, S. Thurgate, K. Prince, *Electrochem. Solid-State Lett.* **2006**, *9*, A471 – A474.
[46] Y. Q. Huang, J. Fang, F. Omenya, M. O'Shea, N. A. Chernova, R. B. Zhang, Q. Wang, N. F. Quackenbush, L. F. J. Piper, D. O. Scanlon, M. S. Whittingham, *J. Mater. Chem. A* **2014**, *2*, 12827 – 12834.
[47] J. Park, H. Kim, K. Jin, B. J. Lee, Y. S. Park, H. Kim, I. Park, K. D. Yang, H. Y. Jeong, J. Kim, K. T. Hong, H. W. Jang, K. Kang, K. T. Nam, *J. Am. Chem. Soc.* **2014**, *136*, 4201 – 4211.
[48] S. Y. Lim, H. Kim, R. A. Shakoor, Y. Jung, J. W. Choi, *J. Electrochem. Soc.* **2012**, *159*, A1393 – A1397.
[49] Y. Jiang, J. A. Shi, M. Wang, L. C. Zeng, L. Gu, Y. Yu, *ACS Appl. Mater. Interfaces* **2016**, *8*, 689 – 695.
[50] J. Yang, H. Wang, P. F. Hu, J. J. Qi, L. Guo, L. H. Wang, *Small* **2015**, *11*, 3744 – 3749.
[51] D. X. Wang, Q. Liu, C. J. Chen, M. L. Li, X. Meng, X. F. Bei, Y. J. Wei, Y. H. Huang, F. Du, C. Z. Wang, G. Chen, *ACS Appl. Mater. Interfaces* **2016**, *8*, 2238 – 2246.
[52] B. V. R. Chowdari, G. V. S. Rao, G. Y. H. Lee, *Solid State Ionics* **2000**, *136*, 1067 – 1075.
[53] F. Lalère, V. Seznec, M. Courty, R. David, J. N. Chotard, C. Masquelier, *J. Mater. Chem. A* **2015**, *3*, 16198 – 16205.

Received: July 5, 2016
Revised: August 4, 2016
Published online: ■■ ■■, ■■■■

Zuschriften

Natriumionenbatterien

H. C. Gao,
J. B. Goodenough* ——— ■■■■–■■■■

An Aqueous Symmetric Sodium-Ion Battery with NASICON-Structured $Na_3MnTi(PO_4)_3$

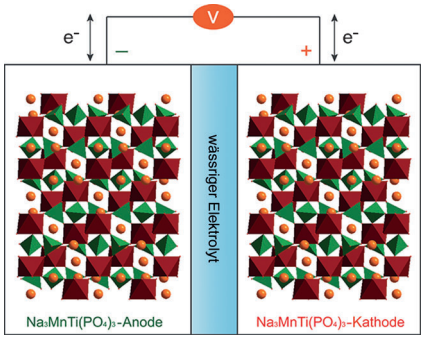

Ein Material für beide Zwecke: Eine wässrige symmetrische Natriumionenbatterie wurde mit dem NASICON-strukturierten $Na_3MnTi(PO_4)_3$ aufgebaut, wobei die Redoxpaare Ti^{4+}/Ti^{3+} und Mn^{3+}/Mn^{2+} auf der Anoden- bzw. Kathodenseite operieren. Die Batterie zeigt gut definierte Spannungsplateaus, die im elektrochemischen Fenster eines wässrigen Elektrolyten positioniert sind, sowie hohe Zyklenstabilität und Ratenkapazität.